A minimal tat system from a gram-positive organism - A bifunctional TatA subunit participates in discrete TatAC and TatA complexes

Barnett, James P.; Eijlander, Robyn T.; Kuipers, Oscar P.; Robinson, Colin

Published in:
The Journal of Biological Chemistry

DOI:
10.1074/jbc.M708134200

Publication date:
2008

THE JOURNAL OF BIOLOGICAL CHEMISTRY VOL. 283, NO. 5, pp. 2534–2542, February 1, 2008

A Minimal Tat System from a Gram-positive Organism

*A BIFUNCTIONAL TatA SUBUNIT PARTICIPATES IN DISCRETE TatAC AND TatA COMPLEXES**

Received for publication, October 1, 2007, and in revised form, November 15, 2007 Published, JBC Papers in Press, November 20, 2007, DOI 10.1074/jbc.M708134200

James P. Barnett[‡1], Robyn T. Eijlander[§1], Oscar P. Kuipers[§], and Colin Robinson[‡2]

From the [‡]Department of Biological Sciences, University of Warwick, Coventry CV4 7AL, United Kingdom and the [§]Department of Molecular Genetics, Groningen Biomolecular Sciences and Biotechnology Institute, University of Groningen, Kerklaan 30, 9751 NN Haren, The Netherlands

The Tat system transports folded proteins across bacterial and thylakoid membranes. In Gram-negative organisms, a TatABC substrate-binding complex and separate TatA complex are believed to coalesce to form an active translocon, with all three subunits essential for translocation. Most Gram-positive organisms lack a *tatB* gene, indicating major differences in organization and possible differences in mode of action. Here, we have studied Tat complexes encoded by the *tatAdCd* genes of *Bacillus subtilis*. Expression of *tatAdCd* in an *Escherichia coli tat* null mutant results in efficient export of a large, cofactor-containing *E. coli* Tat substrate, TorA. We show that the *tatAd* gene complements *E. coli* mutants lacking either *tatAE* or *tatB*, indicating a bifunctional role for this subunit in *B. subtilis*. Second, we have identified and characterized two distinct Tat complexes that are novel in key respects: a TatAdCd complex of ~230 kDa that is significantly smaller than the analogous *E. coli* TatABC complex (~370 kDa on BN gels) and a separate TatAd complex. The latter is a discrete entity of ~270 kDa as judged by gel filtration chromatography, very different from the highly heterogeneous *E. coli* TatA complex that ranges in size from ~50 kDa to over 600 kDa. TatA heterogeneity has been linked to the varying size of Tat substrates being translocated, but the singular nature of the *B. subtilis* TatAd complex suggests that discrete TatAC and TatA complexes may form a single form of translocon.

The Tat (twin arginine translocation) pathway is involved in the transport of proteins across the chloroplast thylakoid membrane and the plasma membranes of a wide range of bacteria (1–6). It differs fundamentally from the other export pathway, the Sec pathway, in its ability to translocate prefolded proteins over the plasma membrane. This process appears not to require energy in the form of ATP hydrolysis but is instead dependent on the presence of the proton motive force across the membrane (1, 7, 8). Substrates for this translocation pathway bear N-terminal signal peptides that contain a highly conserved, characteristic twin-arginine motif in the N-terminal domain of the signal peptide (9–11).

In *Escherichia coli* and other Gram-negative organisms, the above studies have identified three genes as being essential for Tat-dependent protein translocation: *tatA*, *tatB*, and *tatC* (usually in the form of a *tatABC* operon). The three *tat* genes of *E. coli* encode membrane proteins of 9.6, 18.4, and 28.9 kDa in size, respectively. The TatA and TatB proteins are both predicted to contain a single transmembrane spanning domain, whereas the larger TatC protein is predicted to contain six transmembrane-spanning domains (12). These three proteins have been shown to form two main types of complex within the cytoplasmic membrane of *E. coli*. The first is a TatABC complex of ~370 kDa (13, 14), which is thought to be involved in substrate recognition and binding; in particular, substrates appear to interact initially with the TatB and TatC subunits (15, 16). The second form of Tat complex appears to contain only TatA molecules, and whereas the *E. coli* TatABC complex is both discrete and stable, the TatA complexes range in size from less than 100 kDa to over 500 kDa (17, 18). Single-particle electron microscopy reveals the TatA to form ring-like structures of varying diameter (18), prompting suggestions of a role in formation of the translocation pore.

Tat systems in other Gram-negative organisms appear (so far) to conform to a similar pattern, whereas Gram-positive organisms contain very different Tat systems. In virtually every case, with the exception of *Streptomyces* species (19), these organisms contain only *tatAC* genes, indicating fundamental differences between the two types of Tat apparatus. Because TatA and TatB proteins share a degree of sequence homology, one possibility is that the TatA proteins in Gram-positive bacteria are bifunctional, performing the functions of both the TatA and TatB proteins of *E. coli* (20). Alternatively, TatB may perform a function in *E. coli* that is not required in Gram-positive organisms, or the two types of system may differ in other key respects.

In this report we have set out to characterize in detail a Tat system from a Gram-positive organism, *Bacillus subtilis*. This is a nonpathogenic, Gram-positive soil bacterium that secretes high levels of extracellular proteins. *B. subtilis* contains three variants of the *tatA* gene, denoted *tatAd*, *tatAy*, and *tatAc*, together with two variants of *tatC*, denoted *tatCd* and *tatCy*; it lacks a *tatB* gene. Recently studies have shown the presence of two distinct translocases, one involving TatAd and TatCd and the other involving TatAy and TatCy. TatAdCd and TatAyCy display differing substrate specificities (21). The secretion of

* This work was supported by Bacell Tat Machine Grant LSHC-CT2004-05257 from the European Union (to C. R. and O. P. K.) and by a Biotechnology and Biological Sciences Research Council Studentship (to J. P. B.). The costs of publication of this article were defrayed in part by the payment of page charges. This article must therefore be hereby marked "*advertisement*" in accordance with 18 U.S.C. Section 1734 solely to indicate this fact.

[1] These authors contributed equally to this work.

[2] To whom correspondence should be addressed. Tel.: 44-2476-523557; Fax: 44-2476-523568; E-mail: colin.robinson@warwick.ac.uk.

TABLE 1
Plasmids and strains

	Relevant properties	Reference
Plasmids		
pBAD-ABC	pBAD24 derivative containing the *E. coli tatABC* operon; Amp^r	Ref. 13
pBAdCd	pBAD24 derivative containing the *B. subtilis tatAdCd-strep* operon; Amp^r	This study
pEXT-AdCd	pEXT22 derivative containing the *B. subtilis tatAdCd operon*; Kan^r	This study
pBAd-his	pBAD24 derivative containing the *B. subtilis tatAd-his* gene; Amp^r	This study
Strains		
E. coli		
MC1061	F$^-$; *araD*139; Δ (*ara-leu*)7696; Δ (*lac*)X74; *galU*; *galK*; *hsdR*2; *mcrA*; *mcrB*1; *rspL*	Ref. 42
MC4100	F$^-$ Δ*lacU*169 *araD*139 *rpsL*150 *relA*1 *ptsF rbs flbB*5301	Ref. 24
MC4100 Δ*tatABCDE*	*tat* deletion strain	Ref. 4
B. subtilis		
168	*trpC2*	Ref. 43

PhoD, a protein with phosphodiesterase and alkaline phosphatase activity, is completely TatAdCd-dependent (22), and the three genes are part of the *pho*-regulon that is only expressed under phosphate-limiting conditions. No other TatAdCd-dependent proteins have been identified to date. TatAyCy has been shown to form an active translocase for the translocation of YwbN, an iron-dependent DyP-peroxidase (22, 23). The function of the third TatA component, TatAc, remains unknown.

Little is currently known about the organization of the *B. subtilis* Tat proteins within the membrane. Here, we analyze the organization and nature of the complexes formed by the components of the *B. subtilis* TatAdCd pathway. We show that these subunits form an active translocase when expressed in an *E. coli* background, and we furthermore show that TatAd is indeed bifunctional. Finally, we show that the *B. subtilis* Tat complexes have unexpected properties that suggest a new model for Tat-dependent protein transport, involving a single defined translocon rather than a spectrum of size variants.

EXPERIMENTAL PROCEDURES

Bacterial Strains, Plasmids, and Growth Conditions—All of the strains and plasmids used are listed in Table 1. *E. coli* MC4100 (24) was used as the parental strain, and Δ*tatABCDE* (4) has been described previously. Arabinose-resistant derivatives were used as described previously (13). *E. coli* was grown aerobically in Luria broth at 37 °C. *E. coli* was grown anaerobically in Luria broth supplemented with 0.5% glycerol, 0.5% trimethylamine *N*-oxide (TMAO),[3] and 1 μM ammonium molybdate. The media were supplemented with ampicillin to a final concentration of 100 μg/ml and arabinose to 0.5 mM when required. *B. subtilis* was grown in TY (trypton/yeast extract) medium, consisting of bactotryptone (1%; w/v), Bacto yeast extract (0.5%; w/v), and NaCl (1%; w/v), unless indicated otherwise. The media were supplemented with kanamycin (10 μg/ml), chloramphenicol (5 μg/ml), and/or spectinomycin (100 μg/ml).

DNA Techniques—All of the cloning techniques and transformation of *E. coli* were performed as described by Sambrook *et al.* (25). All of the enzymes used were from Roche Applied Science or Fermentas Life Sciences. The PCR was performed using Expand DNA polymerase (Roche Applied Science). For arabinose-inducible overproduction of *B. subtilis* TatAdCd, plasmid pBAdCd was constructed as follows. The *tatAdCd* operon was amplified from *B. subtilis* 168 chromosomal DNA with primers RTEAdF (5′-CGC GTC TCG CAT GTT TTC AAA CAT TGG AAT ACC GGG CTT G-3′) and JJdstrep02 (5′-ATA TTC TAG ATT ATT TTT CAA ACT GTG GGT GCG ACC AAT TCG AAG CGG CCG CCG CTG TTT CTT CC-3′). RTEAdF was designed as such that restriction of the generated *tatAdCd-strep* PCR-amplified fragment with dovetail enzyme Esp3I would create an NcoI overhang to ensure direct cloning in the vector pBAD24. JJdstrep02 was constructed in such a way that a C-terminal *Strep*-tag II (26) (underlined) would be directly attached to *tatCd* during the PCR amplification. pBAdCd was constructed by ligating an Esp3I- and XbaI-cleaved PCR-amplified fragment of *tatAdCd-strep* into NcoI- and XbaI-cleaved pBAD24. For isopropyl β-D-thiogalactopyranoside-inducible overproduction of *B. subtilis* TatAdCd, *tatAdCd-strep* was cut out of pBAdCds with NheI and XbaI and ligated into NheI/XbaI-cut pEXT22 to construct pEXT-AdCd.

For arabinose-inducible overproduction of *B. subtilis* TatAd, plasmid pBAd-His was constructed as follows. The *tatAd* gene was amplified from *B. subtilis* 168 chromosomal DNA with primers RTEAdF (5′-CGC GTC TCG CAT GTT TTC AAA CAT TGG AAT ACC GGG CTT G-3′) and TatAdhis-Xba-R (5′-GCT CTA GAT CAG TGA TGG TGA TGG TGA TGG CCC GCG TTT TTG TCC TGC-3′). TatAdhis-Xba-R was constructed in such a way that a C-terminal His_6 tag (underlined) would be directly attached to *tatAd* during the PCR amplification. pBAd-His was constructed by ligating an Esp3I- and XbaI-cleaved PCR-amplified fragment of *tatAd-His* into NcoI- and XbaI-cleaved pBAD24.

Expression and Purification of the TatAdCd Complex and TatAd Complex—*E. coli* Δ*tatABCDE* cells containing plasmid pBAdCd or pBAd-His were grown aerobically to mid-exponential phase with induction of *tatAdCd* on plasmid pBAdCd and *tatAd* on plasmid pBAd-His using 0.5 mM arabinose. The membranes were isolated as described previously and solubilized in 2% digitonin (13). Solubilized membranes were incubated with 2 μg/ml avidin to block any biotin-containing proteins before application to an equilibrated 2 ml Streptactin affinity column (Institut fur Bioanalytik). The column was washed with eight column volumes of equilibration buffer containing Tris-HCl, pH 8.0, 10% glycerol, 150 mM NaCl, and 0.1% digitonin. Bound protein was eluted from the column in six 1.0-ml fractions

[3] The abbreviations used are: TMAO, trimethylamine *N*-oxide; GFP, green fluorescent protein; BN, blue native.

using the same buffer as above but containing 3 mM desthiobiotin (Sigma). Elution fractions were pooled and concentrated to 250 μl using Vivaspin-4 centrifugal concentrators (molecular weight cut-off, 10,000; Vivascience). The concentrated sample was loaded onto a Superose-6HR gel filtration column (Amersham Biosciences) and was eluted with the equilibration buffer described above. For complete purification of the TatAdCd complex, the sample of solubilized membrane was subjected to Q-Sepharose chromatography before the Streptactin and Superose-6HR chromatography steps; the method was as described in Ref. 13.

SDS-PAGE and Western Blotting—The proteins were separated using SDS-polyacrylamide gel electrophoresis and immunoblotted using specific antibodies to TatAd (kindly provided by J. Müller (27)) and goat anti-rabbit IgG horseradish peroxidase conjugate. The *Strep*-tag II on TatCd was detected directly using a Streptactin-horseradish peroxidase conjugate (Institut fur Bioanalytik). SufI, a Tat-dependent substrate of *E. coli*, was visualized using specific antibodies (kindly provided by T. Palmer). GFP was detected using a specific anti-GFP antibody (Living Colors) followed by goat anti-rabbit IgG horseradish peroxidase conjugate. An ECL detection kit (Amersham Biosciences) was used to visualize the proteins.

Blue Native Polyacrylamide Gel Electrophoresis—Blue native polyacrylamide gel electrophoresis was performed as described previously (28). The membranes were prepared as described above and solubilized in 50 mM Bis-Tris, pH 7.0, 750 mM 6-aminocaproic acid, and 2% (w/v) digitonin. Solubilized membranes and purified protein were loaded and separated on a polyacrylamide gradient gel (5–13%). The proteins were detected by immunoblotting as described above.

TMAO Reductase Activity and TorA-GFP Assays—TMAO reductase activity assay was performed as described previously (13, 29). *E. coli* cells were grown anaerobically until mid-exponential growth phase prior to fractionation into periplasmic, cytoplasmic, and membrane fractions. The cell fractions were loaded and separated on a 10% native polyacrylamide gel that was subsequently assayed for TMAO reductase activity as described previously. For TorA-GFP export assays, a construct comprising the TorA signal peptide linked to GFP (30) was expressed using the pBAD-24 plasmid as previously described (31). For these experiments, TatAdCd was expressed from the compatible pEXT22 vector.

Microscopy—Images were recorded with a Leica DMRE microscope equipped with a Leica TCS SP2 confocal unit and an argon laser. The 488-nm laser line was selected, and the images were recorded with a photomultiplier using the Leica confocal software. The samples were visualized with a 63× oil immersion objective (numerical aperture, 1.4; Leica). The image size is 512 × 512 pixels, and the images were averaged from four successive scans.

RESULTS

Overexpressed TatAdCd Forms an Active Translocation Pathway in E. coli—We set out to determine whether overexpressed TatAdCd can form an active translocation pathway in *E. coli*, to use a single defined background for comparing Tat systems from Gram-negative and Gram-positive organisms.

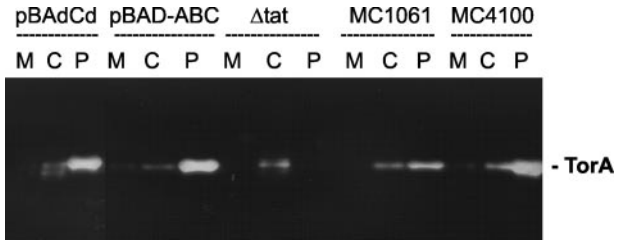

FIGURE 1. **Expression of *B. subtilis* TatAdCd in an *E. coli tat* null mutant leads to efficient export of TorA.** The figure shows a native polyacrylamide gel stained for TMAO reductase (*TorA*) activity. Membrane, cytoplasm, and periplasm samples (*M*, *C*, and *P*, respectively) were prepared and analyzed from two wild type strains of *E. coli* (MC1061 and MC4100 as indicated), from Δ*tatABCDE* cells (Δ*tat*) and from Δ*tatABCDE* cells expressing *E. coli* TatABC from plasmid pBAD-ABC, or *B. subtilis* TatAdCd from plasmid pBAdCd as indicated. The mobility of active TorA is indicated.

The *tatAdCd* genes were expressed in an *E. coli tat* null mutant (Δ*tatABCDE*), and we conducted a TMAO reductase activity assay as described under "Experimental Procedures." TMAO reductase (TorA) is a periplasmic protein required for growth of *E. coli* on a minimal TMAO and glycerol medium. It is a known *E. coli* Tat substrate that is frequently used for Tat export assays because its presence can be detected through an assay using methyl-viologen-linked reduction on a native polyacrylamide gel. TatAdCd was overexpressed from plasmid pBAdCd in Δ*ABCDE* cells under anaerobic conditions, after which the cells were fractionated, and TorA was localized as shown in Fig. 1.

The right-hand sets of lanes in Fig. 1 show control tests in which the wild type *E. coli* strains, MC1061 and MC4100 (from which the Δ*ABCDE* strain was derived) were fractionated into membrane, cytoplasm, and periplasm samples (*lanes M*, *C*, and *P*, respectively). The data show that the TorA activity is localized primarily in the periplasm as expected, with low levels found in the cytoplasm as is often observed (13). In the Δ*ABCDE* strain (denoted Δ*tat*), no periplasmic activity is detected, and TorA is found exclusively in the cytoplasm. Expression of plasmid-borne *E. coli* TatABC in this strain (from the pBAD-ABC vector) restores export activity as expected. The important point is that expression of *B. subtilis* TatAdCd, using the same vector, also leads to efficient export of TorA. Clearly, TatAdCd is able to form an active translocation pathway in the *E. coli* Δ*ABCDE* strain, and this is the first demonstration that a TatAC-type system from a Gram-positive organism can function in a Gram-negative background and export authentic *E. coli* Tat substrates. Moreover, because TatB has been found to be essential for TorA translocation in *E. coli* (32), this strongly suggests that *B. subtilis* TatAd displays both TatA and TatB activity.

Overexpression of TatAdCd Does Not Fully Complement E. coli ΔABCDE Cells in Tat-dependent Substrate Translocation—Although repeated tests consistently showed TatAdCd to be capable of efficiently exporting TorA, it was considered important to analyze its ability to also export other substrates. We first tested whether the cells can export a fusion protein comprising the TorA signal peptide linked to GFP. This fusion is exported by the Tat pathway in *E. coli* (30, 31). We expressed TorA-GFP in *E. coli* Δ*ABCDE* cells and coexpressed *tatAdCd* or *E. coli tatABC* on the compatible pEXT22 plasmid

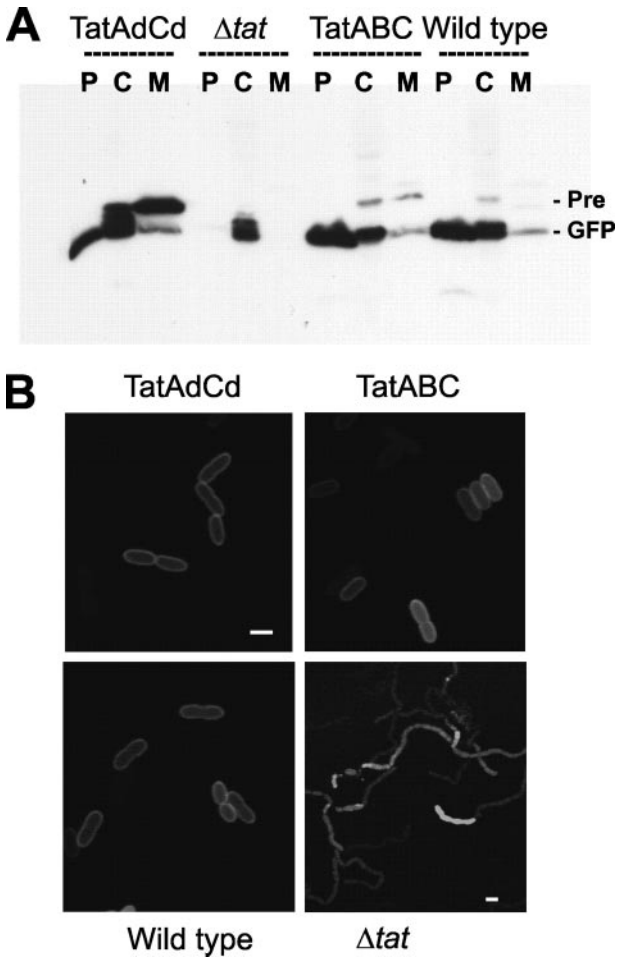

FIGURE 2. **Expression of *B. subtilis* TatAdCd leads to export of TorA-GFP.** A construct comprising the TorA signal peptide linked to GFP (TorA-GFP) was expressed from the pBAD-24 plasmid in wild type MC4100 cells, Δ*tatABCDE* cells (Δ*tat*), and Δ*tatABCDE* cells expressing *E. coli* TatABC or *B. subtilis* TatAdCd (using the compatible pEXT22 plasmid). *A*, cells were fractionated into membrane, cytoplasm, and periplasm samples (*M*, *C*, and *P*, respectively) that were immunoblotted using anti-GFP antibodies. The mobilities of mature size GFP and the precursor form (*Pre*) are indicated. *B*, cells were analyzed by confocal laser microscopy as detailed under "Experimental Procedures." The *scale bar* is 1 μm.

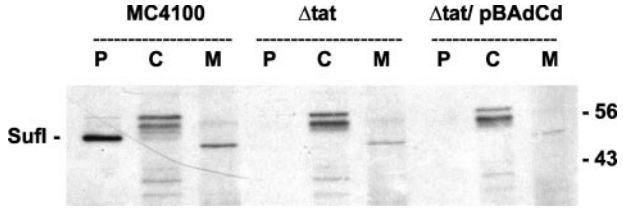

FIGURE 3. **SufI is not transported by *B. subtilis* TatAdCd.** Membrane, cytoplasm, and periplasm samples (*M*, *C*, and *P*, respectively) were prepared and analyzed from wild type *E. coli* cells (MC4100 panel), from Δ*tatABCDE* cells (Δ*tat*) and from Δ*tatABCDE* cells expressing *B. subtilis* TatAdCd from plasmid pBAdCd as indicated. The samples were immunoblotted using antibodies to *E. coli* SufI, the mobility of which is indicated. Mobilities of two molecular mass markers (in kDa) are shown on the *right*.

as detailed under "Experimental Procedures." The cells were fractionated into membrane, cytoplasm, and periplasm fractions, and the data are shown in Fig. 2*A*. In control tests (Fig. 2*A*, *wild type panel*), GFP is found as mature size protein in the periplasm (*P*) when expressed in wild type cells. Some mature size protein is also found in the cytoplasm, but we have observed this phenomenon before and concluded that it is due to proteolytic clipping of the precursor form (31). The TorA-GFP accumulates exclusively in the cytoplasm when expressed in a *tat* null mutant (Δ*tat* panel), again mostly as mature size protein. The remaining panels show that the protein is exported if either *E. coli* TatABC or *B. subtilis* TatAdCd is coexpressed in a Δ*tat* background. High levels of mature protein are present in the periplasm in both cases, confirming efficient export.

These data were confirmed by confocal microscopy of the cells as shown in Fig. 2*B*. Clear periplasmic halos of GFP fluorescence are evident when the TorA-GFP is expressed in wild type cells or in cells expressing TatAdCd or *E. coli* TatABC. In contrast, the fluorescence is purely cytoplasmic when the construct is expressed in Δ*tatABCDE* cells.

Fig. 2*B* also illustrates an important point regarding the ability of the TatAdCd system to export other substrates. Two Tat substrates in *E. coli*, amidase A and C, have been shown to be involved in cytokinesis (33). These substrates are mislocalized in a Δ*ABCDE* deletion strain causing a distorted cell division phenotype; as a result the cells grow in long chain-like filaments (34). The wild type phenotype is clearly restored by complementing the Δ*ABCDE* strain with plasmid-borne TatABC (TatABC image). However, expression of *B. subtilis* TatAdCd also restores the wild type cell division phenotype (*TatAdCd panel*), strongly suggesting that the TatAdCd complex of *B. subtilis* is able to translocate one or both of the amidase A and C proteins.

We also analyzed the translocation of SufI, another authentic *E. coli* Tat substrate, in the *E. coli* Δ*ABCDE* deletion strain complemented with *B. subtilis* TatAdCd (Fig. 3). The mature size, 50-kDa SufI protein is clearly detected in the periplasm (*P*) of wild type MC4100 cells with some precursor protein apparent in the cytoplasmic fraction (*C*). An additional band slightly smaller than mature SufI is also detected in the membrane fraction (*M*), although the significance of this band is unclear. As expected, deletion of the *E. coli* Tat machinery resulted in accumulation of SufI in the cytoplasm (Δ*tat panel*). In this case, export could not be restored by expression of TatAdCd of *B. subtilis* (Δ*tat/pBAdCd panel*), with no SufI detected in the periplasm. We conclude that not all Tat-dependent substrates of *E. coli* can be translocated by this AC-type translocase.

TatAd Is Bifunctional and Able to Complement Both the Δ*tatAE and* Δ*tatB E. coli Mutants*—The absence of a *tatB* gene in most Gram-positive organisms suggests that the Gram-positive TatA subunits are able to carry out both the TatA and TatB roles involved in Tat systems from Gram-negative organisms (20). This important point has not been addressed experimentally, and we therefore expressed *B. subtilis* TatAd in the *E. coli* Δ*tatAE* and Δ*tatB* strains to test whether it can complement the defects. The results (Fig. 4) show that TorA activity is transported to the periplasm when His-tagged TatAd is expressed in either the Δ*tatAE* or Δ*tatB* strains, clearly demonstrating that this subunit is able to execute both the TatA and TatB roles. Note that the signal intensity of the periplasmic TorA band appears to be low when TatAd is expressed in the ΔtatAE strain, but this assay is not quantitative, and from other experiments TatAd complements the two strains to an apparently equal

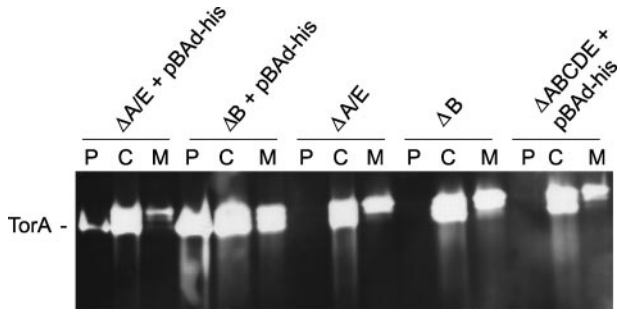

FIGURE 4. ***B. subtilis* TatAd complements both the ΔtatAE and ΔtatB *E. coli* mutants.** His-tagged TatAd was expressed using the pBAd-His vector ("Experimental Procedures") in the *E. coli* Δ*tatAE,* Δ*tatB* and Δ*tatABCDE* mutants as shown. After induction for 3 h in the presence of 0.1 mM arabinose, the cells were fractionated into membrane, cytoplasm, and periplasm samples (*M*, *C*, and *P*, respectively), which were analyzed on a native gel that was stained for TorA activity. Similar fractionations were made using Δ*tatAE* and Δ*tatB* cells in control experiments.

extent (data not shown). In the control sample, no periplasmic TorA activity is detected when TatAd is expressed in a *tat* null mutant strain (Δ*tatABCDE*; the panel is overexposed to detect the cytoplasmic and membrane-bound TorA activity in the *P* and *M lanes*). No export of TorA is evident in the Δ*tatAE* or Δ*tatB* strains either, because Tat activity is absolutely dependent on the presence of TatB plus either TatA or the TatA homolog, TatE (Ref. 4 and data not shown).

Purification of Overexpressed TatAdCd Reveals the Presence of Two Forms of Tat Complex: TatAdCd and TatAd—To analyze the Tat complexes present after expression of *B. subtilis* TatAdCd in *E. coli*, the membranes were solubilized in digitonin, after which the lysate was subjected to Streptactin affinity chromatography utilizing the *Strep*-tag II on the C terminus of TatCd as described under "Experimental Procedures." Column fractions were subjected to immunoblotting using specific antibodies to TatAd and the *Strep*-tag II on TatCd. The data shown in Fig. 5*A* confirm that essentially all of the TatCd-strep had bound to the column; virtually none was detected in the wash fractions. Most of the TatCd-strep was found in elution fractions 2–4, with a clear peak in fraction 3. A small amount of TatAd copurified with the TatCd-strep strongly suggesting the presence of a TatAdCd complex. However, the vast majority of the TatAd did not coelute with the TatCd-strep and was instead detected in the first three wash fractions. This is reminiscent of similar studies on *E. coli* TatABC, with the majority of additional "free" TatA likewise detected in the wash fractions as a separate complex (13). The data thus point to the presence of two types of complex, one composed of TatAdCd and another composed only of TatAd.

To determine the composition of the TatCd/TatAd-containing complex, the elution fractions were subjected to gel filtration chromatography using a Superose-6 matrix, and Fig. 5*B* shows a silver-stained gel of samples from each stage of the overall purification protocol: total membrane starting material, Q-Sepharose chromatography, Streptactin affinity chromatography, and gel filtration chromatography. The final sample shows the presence of only the 25-kDa TatCd subunit. TatAd does not stain well with silver, but its presence was confirmed by immunoblotting (Fig. 5*B*, *left panel*). The TatAdCd complex has thus been purified to homogeneity. Note that the TatAd

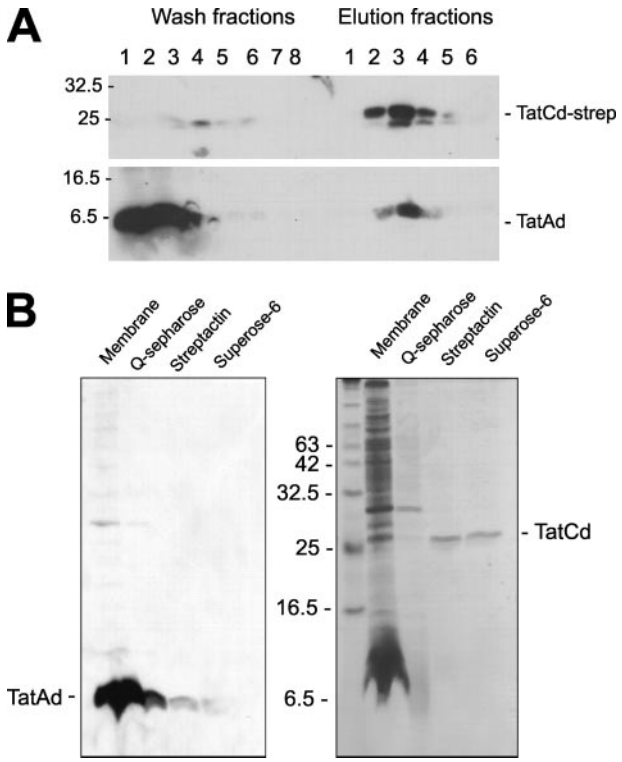

FIGURE 5. **Separation of distinct *B. subtilis* TatAdCd and TatAd-containing complexes, and purification of the *B. subtilis* TatAdCd complex.** *A*, membranes were prepared from Δ*tatABCDE* cells expressing *B. subtilis* TatAdCd (from plasmid pBAdCd as above), solubilized in digitonin and applied to a Streptactin affinity column as detailed under "Experimental Procedures." The figure shows immunoblots of wash (*washes 1–8*) and elution (*elutions 1–6*) fractions using antibodies to the *Strep*-tag II on the C terminus of TatCd (protein is denoted as TatCd-strep) and to TatAd. Mobilities of molecular mass markers (in kDa) are shown on the *left*. *B*, purification of the TatAdCd complex to homogeneity. Solubilized membranes from cells expressing TatAdCd were subjected to Q-Sepharose, Streptactin, and Superose-6HR gel filtration chromatography as detailed under "Experimental Procedures." Samples of each eluate were analyzed on a silver-stained gel (*right panel*) or blotted with antibodies to TatAd (*left panel*). The mobilities of molecular mass markers (in kDa) are shown.

blot of the purified samples is weak compared with the original membrane sample; this reflects the fact that only a very small proportion of the TatAd pool is associated with TatCd.

Highly Discrete TatAdCd and TatAd Complexes—The sizes of the two forms of *B. subtilis* Tat complex were analyzed using calibrated gel filtration chromatography. Digitonin-solubilized membranes from cells expressing TatAdCd-strep were applied to a calibrated Superose-6 gel filtration column as described under "Experimental Procedures," and elution fractions were immunoblotted using antibodies against TatAd and TatCd-strep (Fig. 6*A*). The elution profiles of the TatAdCd and TatAd complexes were quantified by densitometry of the bands, and the graphs are shown in Fig. 6*A*. We also expressed, solubilized, and fractionated the membrane-bound *E. coli* TatABC and TatA complexes under exactly the same conditions for comparison, and we analyzed the TatA-type complexes extracted from the cytoplasm (also indicated in Fig. 6*B*). The data show that TatCd elutes in fractions 20–27, and TatAd elutes in fractions 22–26. Quantification of the intensity of the bands reproducibly shows that TatCd is eluting with a peak in fraction 23 corresponding to a molecular mass of ~350

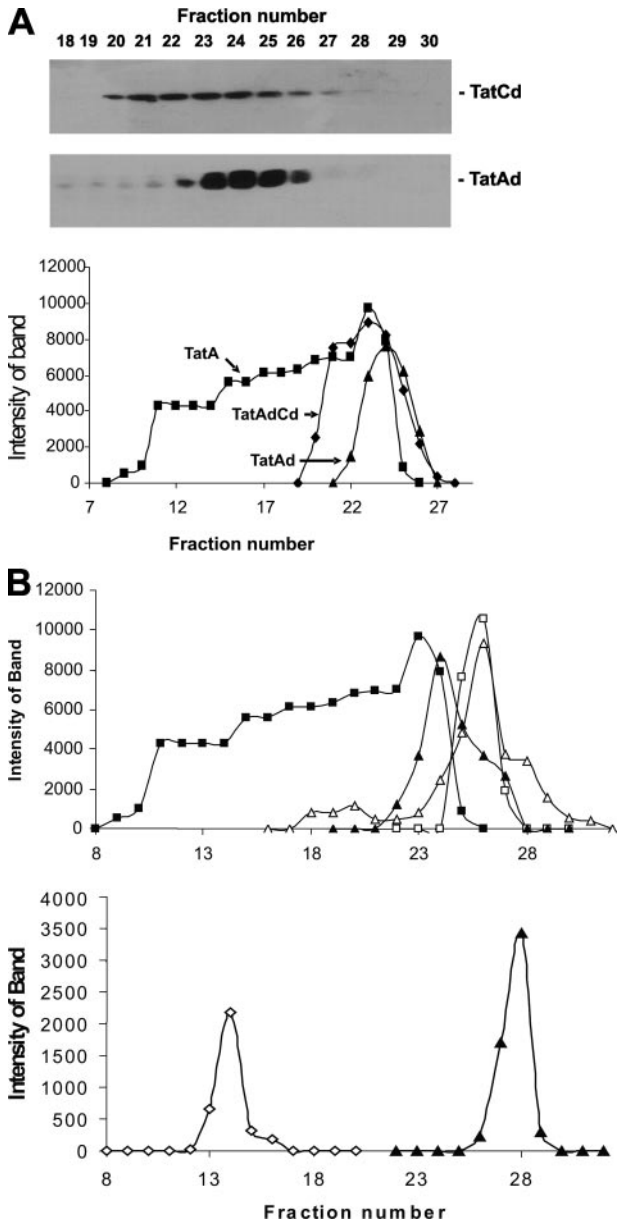

FIGURE 6. **TatAdCd and TatAd are discrete complexes that differ from their *E. coli* counterparts.** *A*, digitonin-solubilized membranes from cells expressing TatAdCd (as in above figures) or *E. coli* TatABC were applied to a calibrated Superose-6HR column. Peak elution fractions were analyzed by immunoblotting using antibodies to the *Strep*-tag II (on TatCd) or TatAd as indicated. The immunoblots were analyzed by densitometry (of the entire set of elution fractions), and the intensities of the bands are shown plotted against fraction number. TatAdCd and TatAd elution are denoted by *black diamonds* and *black triangles*, respectively. The elution of *E. coli* TatA complexes was analyzed under identical conditions and is shown in the same graph (*squares*). *B*, fractionation of membrane-bound and cytosolic TatAd. *Upper graph*, TatAdCd was expressed as in A and membranes were solubilized in 1% digitonin as in A, or 1% octyl glucoside or 1% dodecyl maltoside and subjected to Superose 6 chromatography in the same detergent. The graph shows the elution of TatAd in digitonin (*black triangles*), octyl glucoside (*white triangles*), or dodecyl maltoside (*white squares*). The elution of digitonin-solubilized *E. coli* TatA is also illustrated for comparative purposes (*black squares*). The *lower graph* of *B* shows the fractionation of cytosolic TatAd. Here, TatAdCd were expressed as in A (with TatAd untagged), or with a His_6 tag attached to the C terminus of TatAd using the vector pBAd-his. After lysis of the cells, the cytosolic fraction was subjected to Superose 6 gel filtration chromatography as in *A* but without detergent present at any step. The fractions were immunoblotted for TatAd, and the graph illustrates the elution profiles for untagged and His-tagged TatAd (*white diamonds* and *black triangles*, respectively).

kDa, whereas the bulk of the TatAd elutes later with a peak in fraction 24, which corresponds to a molecular mass of ~270 kDa. Given that the vast majority of TatAd is not bound to TatCd (above), the data indicate the presence of a ~350-kDa TatAdCd complex and a ~270-kDa TatAd complex. These figures include the digitonin micelle, which contributes substantially to the size estimate (28).

For comparison, we expressed *E. coli* TatABC using the same expression system and solubilized the membranes using the same protocol. When subjected to gel filtration chromatography under identical conditions, *E. coli* TatA elutes across a much broader range of fractions than does TatAd, reflecting the enormous range of sizes determined for this complex (13, 28, 29). In contrast, the *B. subtilis* TatAd elutes with a far sharper peak, which clearly indicates the presence of a complex that is both smaller and far more homogeneous than the *E. coli* counterpart.

Digitonin forms particularly large micelles, so for a more accurate estimation of the size of the TatAd complex, we expressed TatAd alone and solubilized the membranes in either dodecyl maltoside or octyl glucoside prior to fractionation in the same detergent (Fig. 6*B*, *upper graph*, *white squares* or *triangles*, respectively). In both cases the TatAd complex elutes later than when solubilized in digitonin (*black triangles*), presumably because of the much smaller micelle size. In both dodecyl maltoside and octyl glucoside, TatAd elutes at a position that corresponds to a mass of 160 kDa, which we assume to be a more accurate reflection of the complex size (although the micelle will still contribute to a degree).

Cytosolic TatAd Is Present as Very Large Aggregates—Although studies on the *E. coli* and thylakoid systems have focused on roles of membrane-bound TatABC proteins, recent studies on the *B. subtilis* TatAdCd system have suggested a completely different mode of action in which the precursor of PhoD is initially recognized by TatAd in the cytosol (27, 35, 36). This would differ dramatically from the *E. coli* and thylakoid systems, where substrates bind to a membrane-bound TatBC dimer (15, 16). Having characterized the size properties of membrane-bound TatAd when expressed in *E. coli*, we therefore tested whether TatAd is also present in the cytosol. This was done after expression of two forms of TatAd, an untagged version of TatAd (using the plasmid pBAdCd as in the above studies) and one with a His_6 tag present on the C terminus of TatAd (pBAd-His plasmid). The two forms were expressed using the pBAD24 vector, and the cytosolic fraction was subjected to Superose 6 gel filtration chromatography (Fig. 6*B*, *lower graph*). The data show that the untagged TatAd is present as very large multimeric forms. The protein elutes in fraction 14 (*white diamonds*), which corresponds to an average size of ~2 MDa. Surprisingly, the presence of a His tag causes a huge change of structure, and the protein elutes much later from the column, at a position corresponding to a size of ~200 kDa (similar to that observed in Ref. 27). These data do raise questions about the significance of the cytosolic TatAd, and this issue is discussed below.

Blue Native Gel Electrophoresis Shows the Presence of a ~230-kDa TatAdCd Complex—To analyze the purified TatAdCd and TatAd complexes further, blue native (BN) polyac-

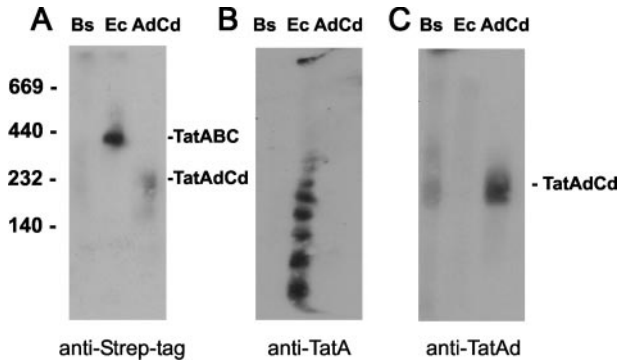

FIGURE 7. **Blue native gel electrophoresis identifies a discrete TatAdCd complex with an estimated mass of ~230 kDa.** Samples of Δ*tatABCDE* cells expressing *E. coli* TatABC (*lanes Ec*) or *B. subtilis* TatAdCd (*lanes Bs*), and samples of purified TatAdCd (*lane AdCd*; see Fig. 5) were subjected to blue native gel electrophoresis as described under "Experimental Procedures." The gel was immunoblotted using antibodies to the *Strep*-tag II on the C termini of TatC/TatCd (*A*), to *E. coli* TatA (*B*), or TatAd (*C*). Mobilities of molecular mass markers (in kDa) are indicated on the *left*, and the mobilities of *E. coli* TatABC and *B. subtilis* TatAdCd are also indicated.

rylamide gel electrophoresis was utilized according to the method described under "Experimental Procedures" (Fig. 7). Gel filtration chromatography provides a reasonable estimate of complex size, but it is heavily affected by the size of detergent micelles. To circumvent this effect and obtain a more accurate description of the complexes, purified TatAdCd and solubilized membranes expressing TatAdCd were run on a blue native polyacrylamide gel. This gel system has been specifically developed for the analysis of membrane protein complexes because it effectively removes the bias caused by the detergent micelles. Digitonin-solubilized membranes from cells expressing *B. subtilis* TatAdCd-strep (*lanes Bs*), *E. coli* TatABC (*lanes Ec*), or purified *B. subtilis* TatAdCd-strep (*lanes AdCd*) were loaded onto a BN gel. The gels were subjected to Western blotting followed by immunodetection with antibodies against the *Strep*-tag II (Fig. 7*A*), *E. coli* TatA (Fig. 7*B*), and *B. subtilis* TatAd (Fig. 7*C*).

Reproducing earlier findings (17), the *E. coli* TatABC complex was visualized as a band comigrating with the marker band of 440 kDa using antibodies against the *Strep*-tag II (Fig. 7*A*, *lane Ec*). Previous studies have shown that, after careful calibration of this gel system, the actual size of this complex is ~370 kDa as judged by this technique (28). Analysis of purified *B. subtilis* TatAdCd complex (prepared as described above) reveals a band that comigrates with the 232-kDa marker. A band of the same size is detected when the same blot is probed with antibodies to TatAd (Fig. 7*C*), confirming that this band corresponds to a TatAdCd complex of ~230 kDa. A band of similar size is evident in samples of whole membranes taken from cells expressing TatAdCd (*lane Bs*), although it is less clear, and some smearing is evident. However, because essentially all of the TatAdCd complex binds to the Streptactin affinity matrix, and only the ~230-kDa TatAdCd complex is detected, we are confident that this is the major species of TatAdCd complex present in the membrane.

Fig. 7*B* clearly shows the "ladder" of differently sized *E. coli* TatA complexes, but it has not been possible to study the *B. subtilis* TatAd complex using BN gels. Although the TatAd antibodies clearly detect the purified TatAdCd complex in Fig. 7*C* (*lane AdCd*), there is no clear additional band in the whole membrane sample (*lane Bs*) from cells expressing TatAdCd. It is possible that the TatAd complex is too small for accurate analysis using the BN system under these conditions.

DISCUSSION

A wealth of data have emerged from studies on the TatABC and TatA complexes of Gram-negative bacteria (particularly *E. coli*) as well as the corresponding plant thylakoid complexes (Hcf106-TatC complex and homo-oligomeric Tha4 complexes). In most respects, the *E. coli* and plant systems appear to operate by broadly similar mechanisms in which two key points are considered to be noteworthy. First, cross-linking data point to the presence of a membrane-bound substrate-binding complex in which TatB and TatC play critical roles (15, 16). A tight association between these components has been confirmed by one study that showed a translational TatB-TatC fusion to be active (13). Second, the available evidence indicates that a TatA (or Tha4) complex assembles and exists as a separate entity and appears to be recruited by the TatABC (or plant Hcf106-TatC complex) only at the point of translocation (37).

In this study we have sought to study Tat complexes from the Gram-positive organism *B. subtilis*. The absence of *tatB* genes in the majority of Gram-positive organisms clearly indicates that their Tat systems differ significantly from the *E. coli* model, and it is important to identify similarities and differences (particularly any mechanistic differences) between the two types of system. In this context, our data are important because they show for the first time that an authentic *E. coli* Tat substrate, TorA, can be effectively transported by the *B. subtilis* TatAdCd system. This indicates that there are no system-specific factors in *B. subtilis* that are required for this system to operate, which could be absent in Gram-negative organisms. This focuses attention on the TatAdCd subunits as the critical components.

The absence of a *tatB* gene in *B. subtilis* raises the possibility that TatA is bifunctional in Gram-positive bacteria, fulfilling the roles of both TatA and TatB from Gram-negative organisms (20). This possibility is backed up by the recent demonstration (38) that selective mutations in *E. coli* TatA can enable it to carry out both TatA and TatB functions. In this report we have provided experimental confirmation of the bifunctional nature of TatAd; this subunit can complement both the Δ*tatAE* and Δ*tatB E. coli* mutants. TatA and TatB play completely different roles in the *E. coli* Tat system (1, 2, 13, 15, 18), which clearly indicates a dual role for TatAd in the *B. subtilis* TatAC-type mechanism.

When compared with the *E. coli* Tat complexes, the *B. subtilis* Tat complexes exhibit important common features but also significant differences. The primary common feature is the presence of two distinct Tat complexes. We have shown that expression of the *B. subtilis tatAdCd* genes results in the presence of separate membrane-bound TatAdCd and TatAd complexes, and these results are very reminiscent of findings on the *E. coli* system where separate TatABC and TatA complexes are present at steady state (13, 17, 18).

However, the *B. subtilis* Tat complexes encoded by *tatAdCd* differ from their *E. coli* counterparts in three important

respects. One of these has already been noted: the absence of TatB in the core substrate-binding complex; its position appears to be occupied by TatAd. The second relates to the nature of the TatAdCd complex; like the *E. coli* TatABC complex, the TatAdCd purifies as a highly discrete entity, but our data indicate that the *B. subtilis* TatAdCd complex is significantly smaller than its *E. coli* counterpart: 230 kDa compared with 370 kDa for the *E. coli* complex as estimated previously by BN gels (17). This may have implications for the number and/or organization of the TatC-containing domains, although it should be noted that an individual TatAdCd domain is smaller than an equivalent *E. coli* TatABC domain (~35 kDa compared with 56 kDa, assuming equimolar stoichiometry as observed for TatBC in the *E. coli* complex (13)).

The third and perhaps most significant difference concerns the TatA complexes. The *E. coli* TatA complex exists as a remarkably heterogeneous set of complexes that range in size from ~50 kDa to well over 500 kDa (17, 18), and this heterogeneity can be clearly visualized as a striking ladder of bands on BN gels. In the above studies it was proposed that this heterogeneity could provide the flexibility for this system to assemble active translocons of differing sizes, which would be logical if a wide range of substrates are to be accommodated without compromising membrane integrity. In contrast, the *B. subtilis* complex is highly discrete in nature; there is no evidence for heterogeneity among the complexes isolated. Nevertheless, this combination of TatAdCd and TatAd complexes is able to transport substrates of very differing sizes, such as authentic TorA (85 kDa) and GFP (25 kDa), as well as its original PhoD substrate in *B. subtilis* (62.5 kDa). On the basis of these data, we believe that the active translocon may be a singular unit capable of accommodating substrates that differ dramatically in terms of size and shape. This would, of course, require real flexibility within the active translocation complex. This scenario would raise questions about the functional significance of the *E. coli* TatA heterogeneity but would be consistent with our observation that the TatA size spectrum is identical in cells that are completely unable to export proteins via this pathway (39).

The TatAdCd complex is furthermore surprisingly small; the size exclusion chromatography estimate is ~160 kDa, and the detergent micelle probably accounts for some of this estimate. These data have interesting implications for the translocation mechanism because TatAdCd is capable of exporting TorA, which is one of the larger Tat substrates (85 kDa). If, as proposed, the active Tat translocon is generated by the coalescence of a TatABC and TatA complex, the sizes of the *E. coli* complexes have been deemed to be consistent with this model (for example, an active translocon of up to 1 MDa in size could be generated by fusion of one of the largest TatA complexes with the 370-kDa TatABC complex). It is less clear whether a substrate of this size can be transported in a folded state by a translocon comprising a 270-kDa TatAdCd complex and 160-kDa TatAd complex. Therefore, it may be the case that the actual translocation process is more complicated than currently imagined, perhaps involving the recruitment of several TatA or TatAd (or even several TatABC or TatAdCd) complexes in both Gram-negative and Gram-positive bacteria.

Finally, it is useful to consider these data in the light of other studies on Tat systems from Gram-positive organisms. Recent studies on the *B subtilis* TatAdCd system (27, 35, 36) suggest a translocation mechanism that is very different from any current model for the *E. coli* or thylakoid Tat system. These studies showed that TatAd can be detected as cytoplasmic oligomers of ~250 kDa, and these oligomers were shown to be able to bind the precursor form of PhoD, the natural substrate of TatAdCd (a membrane-bound form of TatAd is also present in *B. subtilis*). The authors proposed that cytosolic TatAd acts as a soluble receptor for substrate, after which the membrane-bound TatCd recognizes this cytosolic assembly and assists in its membrane integration. More confusingly still, studies on *Streptomyces lividans* (one of the few Gram-positive organisms containing *tatABC* genes) have shown that both TatA and TatB can be detected in the cytoplasm, and the authors proposed that a cytosolic TatAB complex binds substrates and delivers them to TatC (40). These models are fundamentally different in key respects to current models for the Tat system in Gram-negative bacteria and plant thylakoids, where the Tat components are only active in the membrane (13, 15–18).

Although our aim in this study was to analyze the potentially bifunctional TatAd protein and the complexes formed by TatAdCd expression, our data do have relevance to this ongoing debate about Tat mechanism(s) and whether they do indeed differ so diametrically in Gram-negative and Gram-positive organisms. First, we have shown that the TatAd subunit carries out both TatA-like and TatB-like roles in *E. coli*, and because these subunits are believed to function in the membrane in *E. coli*, it is logical to assume that TatAd likewise carries out these functions as a transmembrane protein. Second, we have shown that the TatAdCd system can transport TorA and a TorA-GFP fusion protein, and there is firm evidence that a basically similar TorA fusion protein interacts with a membrane-bound TatBC-containing complex in *E. coli*. Cross-linking studies with a construct comprising the TorA signal peptide linked to a thylakoid lumen passenger protein (41) have shown that the TorA signal peptide specifically binds to a membrane-bound TatBC heterodimer as previously shown for another Tat precursor protein, SufI (15). We have shown that TorA-GFP is capable of using the *B. subtilis* TatAdCd apparatus instead, and it thus seems probable that it interacts with a membrane-bound TatAdCd complex (which we have shown to be present) rather than following a completely different export pathway involving the binding of a soluble TatAd complex. Nevertheless, these are indirect forms of evidence and different, more direct approaches are required to determine whether TatAd functions in the membrane, the cytoplasm, or both.

Acknowledgment—We thank Dr. Anja Nenninger for assistance with the confocal microscope.

REFERENCES

1. Robinson, C., and Bolhuis, A. (2004) *Biochim. Biophys. Acta.* **1694,** 135–147
2. Dalbey, R. E., and Kuhn, A. (2000) *Annu. Rev. Cell Biol.* **16,** 51–67
3. Rodrigue, A., Chanal, A., Beck, K., Muller, M., and Wu, L. F. (1999). *J. Biol. Chem.* **274,** 13223–13228
4. Sargent, F., Bogsch, E. G., Stanley, N. R., Wexler, M., Robinson, C., Berks, B. C., and Palmer, T. (1998). *EMBO J.* **17,** 3640–3650

5. Santini, C. L., Ize, B., Chanal, A., Muller, M., Giordano, G., and Wu, L. F. (1998) *EMBO J.* **17,** 101–112
6. Weiner, J. H., Bilous, P. T., Shaw, G. M., Lubitz, S. P., Frost, L., Thomas, G. H., Cole, J. A., and Turner, R. J. (1998) *Cell* **93,** 93–101
7. Cline, K., Ettinger, W. F., and Theg, S. M. (1992) *J. Biol. Chem.* **267,** 2688–2696
8. Santini, C. L., Ize, B., Chanal, A., Muller, M., Giordano, G., and Wu, L. F. (1998) *EMBO J.* **17,** 101–102
9. Chaddock, A. M., Mant, A., Karnauchov, I., Brink, S., Herrmann, R. G., Klosgen, R. B., and Robinson, C. (1995). *EMBO J.* **14,** 2715–2722
10. Stanley, N. R., Palmer, T., and Berks, B. C. (2000). *J. Biol. Chem.* **275,** 11591–11596
11. Berks, B. (1996) *Mol. Microbiol* **22,** 393–404
12. Behrendt, J., Standar, K., Lindenstrauss, U., and Bruser, T. (2004) *FEMS Microbiol. Lett.* **234,** 303–308
13. Bolhuis, A., Mathers, J. E., Thomas, J. D., Barrett, C. M., and Robinson, C. (2001) *J. Biol. Chem.* **276,** 20213–20219
14. Oates, J., Mathers, J., Mangels, D., Kuhlbrandt, W., Robinson, C., and Model, K. (2003) *J. Mol. Biol.* **330,** 277–286
15. Alami, M., Luke, I., Deitermann, S., Eisner, G., Koch, H. G., Brunner, J., and Muller, M. (2003) *Mol. Cell* **12,** 937–946
16. Cline, K., and Mori, H. (2001) *J. Cell Biol.* **154,** 719–729
17. Oates, J., Barrett, C. M., Barnett, J. P., Byrne, K. G., Bolhuis, A., and Robinson, C. (2005) *J. Mol. Biol.* **246,** 295–305
18. Gohlke, U., Pullan, L., McDevitt, C. A., Porcelli, I., de leeuw, E., Palmer, T., Saibil, H. R., and Berks, B. C. (2005) *Proc. Natl. Acad. Sci. U. S. A.* **102,** 10482–10486
19. Schaerlaekens, K., Schierova, M., Lammertyn, E., Geukens, N., Anne, J., and Van Mellaert, L. (2001) *J. Bacteriol.* **183,** 6727–6732
20. Jongbloed, J. D., van der Ploeg, R., and van Dijl, J. M. (2006). *Trends Microbiol.* **14,** 2–4
21. Jongbloed, J. D., Grieger, U., Antelmann, H., Hecker, M., Nijland, R., Bron, S., and van Dijl, J. M. (2004) *Mol. Microbiol.* **54,** 1319–1325
22. Jongbloed, J. D., Martin, U., Antelmann, H., Hecker, M., Tjalsma, H., Venema, G., Bron, S., van Dijl, J. M., and Muller, J. (2000) *J. Biol. Chem.* **275,** 41350–41357
23. Sturm, A., Schierhorn, A., Lindenstrauss, U., Lilie, H., and Bruser, T. (2006) *J. Biol. Chem.* **281,** 13972–13978
24. Casadaban, M. J., and Cohen, S. N. (1979) *Proc. Natl. Acad. Sci. U. S. A.* **76,** 4530–4533
25. Sambrook, J., Fritsch, E. F., and Maniatis, T. (1989) *Molecular Cloning: a Laboratory Manual*, 2nd Ed., Cold Spring Harbor Laboratory, Cold Spring Harbor, NY
26. Voss, S., and Skerra, A. (1997) *Protein Eng.* **10,** 975–982
27. Pop, O., Martin, U., Abel, C., and Muller, J. P. (2002) *J. Biol. Chem.* **277,** 3268–3273
28. Oates, J., Barrett, C. M. L., Barnett, J. P., Byrne, K. G., Bolhuis, A., and Robinson, C. (2005) *J. Mol. Biol.* **346,** 295–305
29. Silvestro, A., Pommier, J., Pascal, M. C., and Giordano, G. (1989) *Biochim. Biophys. Acta* **999,** 208–216
30. Thomas, J. D., Daniel, R. A., Errington, J., and Robinson, C. (2001) *Mol. Microbiol,* **39,** 47–53
31. Barrett, C. M. L., Ray, N., Thomas, J. D., Robinson, C., and Bolhuis, A. (2003) *Biochem. Biophys. Res. Commun.* **304,** 279–284
32. Sargent, F., Stanley, N. R., Berks, B. C., and Palmer, T. (1999) *J. Biol. Chem.* **274,** 36073–36082
33. Bernhardt, T. G., and de Boer, P. A. (2003) *Mol. Microbiol.* **48,** 1171–1182
34. Ize, B., Stanley, N. R., Buchanan, G., and Palmer, T. (2003) *Mol. Microbiol.* **48,** 1183–1193
35. Schreiber, S., Stenge, R., Westermann, M., Volkmer-Engert, R., Pop, O., and Muller, P. M. (2006) *J. Biol. Chem.* **281,** 19977–19984
36. Westermann, M., Pop, O. I., Gerlach, R., Appel, T. R., Schlormann, W., Schreiber, S., and Muller, J. P. (2006) *Biochim. Biophys. Acta.* **1758,** 443–451
37. Mori, H., and Cline, K. (2002) *J. Cell Biol.* **157,** 205–210
38. Blaudeck, N., Kreutzenbeck, P., Muller, M., Sprenger, G. A., and Freudl, R. (2005) *J. Biol. Chem.* **280,** 3426–3432
39. Barrett, C. M. L., Mangels, D., and Robinson, C. (2005) *J. Mol. Biol.* **347,** 453–463
40. De Keersmaeker, S., Vranken, K., Van Mellaert, L., Anné, J., and Geukens, N. (2007) *Microbiology* **153,** 1087–1094
41. Holzapfel, E., Eisner, G., Alami, M., Barrett, C. M. L., Buchanan, G., Lüke, I., Betton, J.-M., Robinson, C., Palmer, T., Moser, M., and Müller, M. (2007) *Biochemistry* **46,** 2892–2898
42. Wertman, K. F., Wyman, A. R., and Botstein, D. (1986) *Gene* (*Amst.*) **49,** 253–262